Chinese Journal of Aeronautics, (2016), 29(4): 1151–1158

Chinese Society of Aeronautics and Astronautics
& Beihang University

Chinese Journal of Aeronautics

cja@buaa.edu.cn
www.sciencedirect.com

Effect of sodium tartrate concentrations on morphology and characteristics of anodic oxide film on titanium alloy Ti–10V–2Fe–3Al

Ma Kun [a], Yu Mei [a,*], Liu Jianhua [a], Li Songmei [a], Wu Liang [b], Yao Wenhui [a]

[a] School of Materials Science and Engineering, Beihang University, Beijing 100083, China
[b] School of Materials Science and Engineering, Chongqing University, Chongqing 400044, China

Received 6 July 2015; revised 25 July 2015; accepted 6 August 2015
Available online 2 November 2015

KEYWORDS

Anodic oxidation;
Coefficient of friction;
Concentrations;
Corrosion resistance;
Sodium tartrate

Abstract The effect of sodium tartrate concentrations on morphology and characteristics of anodic oxide film on titanium alloy was investigated. The alloy substrates were anodized in different concentration solutions of sodium tartrate with the addition of PTFE emulsion and their morphology and characteristics were analyzed. The anodic oxide film presented a uniform petaloid drums and micro-cracks morphology. Additionally, micro-cracks dramatically swelled with the increase of the tartrate concentrations. The thickness of the anodic oxide film increased with the concentrations until the concentration reached 15 g/L. The results of Raman analysis illustrate that all samples have similarity in the crystal structure, consisting of mainly amorphous TiO_2, some anatase TiO_2 and a small amount of rutile TiO_2. And the ratios of anatase TiO_2 and rutile TiO_2 increase with the concentrations until it reaches 15 g/L. Furthermore, the intensity of the peaks increases with enhanced concentrations until the concentration reaches 15 g/L. The corrosion resistance of the anodic oxide film is increased by the sodium tartrate with higher concentrations before 15 g/L. The coefficient of friction of the anodic oxide film reduces with the concentrations until the concentration reaches 15 g/L, then the coefficient of friction of the anodic oxide film increases with the concentrations.

1. Introduction

Thick, oxide-based film with potential for protection and functionalization of the surface can be obtained by anodization of titanium.[1–3] The anodic oxidation of the anodic oxide film reveals that their property largely depends on the concentrations, electrical source and temperature.[4–6] These factors have been widely researched in recent years.[7–9]

* Corresponding author. Tel.: +86 10 82317103.
E-mail address: yumei@buaa.edu.cn (M. Yu).

Peer review under responsibility of Editorial Committee of CJA.

Production and hosting by Elsevier

http://dx.doi.org/10.1016/j.cja.2015.10.013

Due to the specific behavior of the incorporated anions, the morphology and crystallinity of the oxide layer are affected by concentrations in terms of the change of anodizing forming voltage.[10] Ohtsu et al. reported that high-concentration electrolyte crystallized the oxide layer as a result of the field crystallization effect.[11] In addition, electrolyte affected both the surface morphology and the crystallinity of the fabricated oxide layer.[12,13] Thus, the morphology, microstructure and corrosion resistance of the oxide layer are determined primarily by the electrolyte used. Sodium tartrate is the alkalescent electrolyte that is less destructive to the anodic oxide film. Therefore, sodium tartrate is the electrolyte widely used for anodic oxidation of Ti and alloys for the strong complexation to Ti. However, the effect of the sodium tartrate concentrations on the anodic oxide film is not clear. In this paper, anodic oxide film was fabricated on the Ti–10V–2Fe–3Al by using a pulse galvanostatic method.[14–17] As addition of the sodium tartrate, PTFE particles would obviously improve the corrosion resistance and wear resistance of anodic oxide film.

Thus, the purpose of this paper is to study the effect of sodium tartrate concentrations on morphology and characteristics of anodic oxide film on titanium alloy Ti–10V–2Fe–3Al by AC pulse power supply in the sodium tartrate with the addition of PTFE emulsion. And the mechanism of the enhancement of the properties of the anodic oxide film has been studied in detail. This paper can offer a theoretical of basis for the research in the future.

2. Experimental

2.1. Preparation of anodic oxide film

Titanium alloy Ti–10V–2Fe–3Al was cut into sheets with the dimension of 10 mm × 10 mm × 2 mm. Prior to anodization, samples were polished with silicon carbide paper which successively grades from 200 to 2000 grit followed by rinsing with acetone and deionized water successively and finally dried in air.

Anodic oxidation was carried out in a cell with a thermostat water bath and a magnetic stirring apparatus by using a pulse galvanostatic power source (WMY-IV). The output mode of the power source is pulsed power supply, shown in Fig. 1. In the figure, I is the current, t the time of anodization, T the time of pulse cycle, t^+ the time of pulse working period, and I^+ the pulse anodic current supplied. The Ti–10V–2Fe–3Al slice sample was used as anode, and a 1Cr18Ni9Ti stainless steel plate was used as cathode. The anode surface was less than 50% that of the cathode. The parameters of anodization process are given in Table 1. After the treatment, the coated samples were rinsed with water and then dried in the air.

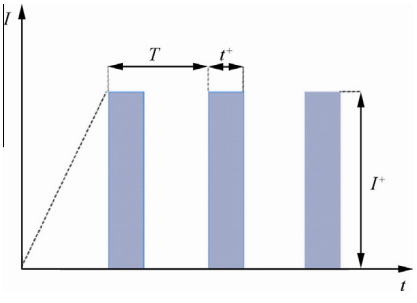

Fig. 1 Output mode of power source.

2.2. Morphology and microstructure of anodic oxide film

The surface morphology and thickness of the anodic oxide film were examined by using scanning electron microscopy (FE-SEM, XL30S, FEI, USA) and atomic force microscope (AFM, Dimension icon, Veeco, USA). The crystalline structure of anodic oxide film was determined by Raman spectroscopy (Raman, Horiba-HR800, Yvon Jobin, using a He-Ne laser without filter, 633 nm).

2.3. Corrosion resistance properties of anodic oxide film

Electrochemical tests were progressed in a traditional three-electrode system (an SCE as reference electrode, a platinum electrode as counter electrode and the oxide sample as working electrode) by using a potentiostat/galvanostat (AES, Parstat 2273, Princeton Applied Research, USA) in a 3.5% NaCl solution. The scanning rate was 0.5 mV · s^{-1} and the scanning range was from −0.5 V to +0.5 V versus the open circuit potential.

2.4. Wear resistance properties of anodic oxide film

Ball disc wear experiments were progressed by using a micro friction and wear machine (UMT-2, CTER, USA). All experiments were carried out by setting the force 3 N for 500 s and the rotation rate was 200 r/min. The diameter of Si_3N_4 grinding ball was 2 mm while diameter of friction being 8 mm. The results were characterized by coefficients of friction of the anodic oxide film.

3. Results and discussion

3.1. Effect of concentrations on thickness

The cross-section images of the anodic oxide film fabricated at different concentrations are shown in Fig. 2 (ρ is the mass of solute per unit volume).

The corresponding thicknesses of the anodic oxide film are 15.7, 16.6, 19.3, 19.4, 19.4 μm respectively, when the concentrations are 1, 5, 15, 30, 50 g/L (Table 2). It was obvious that the thickness of the anodic oxide film would increase with the concentrations until the concentration reached 15 g/L. Thickness of the anodic oxide film would be related to ultimate voltage[18,19] and the rate of the formation and corrosion of the anodic oxide film because of the weak alkaline of electrolyte.[20] At the beginning of the anodic oxidation, the rate of the

Table 1 Parameters of fabrication process.

Parameter	Value
Current density (A · dm^{-2})	5
Sodium tartrate solutions (g · L^{-1})	1, 5, 15, 30, 50
PTFE concentration(mL · L^{-1})	15
Anodization time (min)	40
Duty ratio (%)	20
Frequency (Hz)	1.3

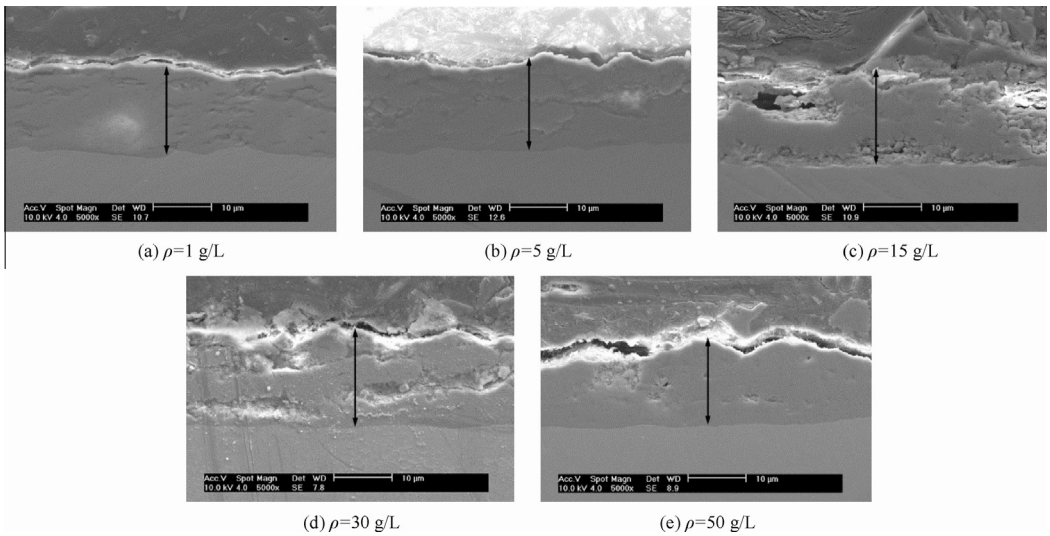

Fig. 2 Cross-section images of anodic oxide film surface obtained at different concentrations of sodium tartrate.

Table 2 Thicknesses of anodic oxide film fabricated at different concentrations.

Concentration (g/L)	Thickness (μm)
1	15.7
5	16.6
15	19.3
30	19.4
50	19.4

formation of anodic oxide film played a dominant role due to the good conductivity of alloy substrate. At this stage, the rate of formation was obviously fast before 5 min according to Fig. 3. As the anode oxidation continued, the anodic oxide film would be too thick to keep the frequent formation for the insulativity of both the anodic oxide film and the PTFE particles. Simultaneously, the anodic oxide film would be corroded by the alkalescent electrolyte leading to the dissolution of it. When the rate of formation equaled to the rate of dissolution, the thickness of anodic oxide film would no longer increase.

The ultimate voltage of the anode oxidation is shown in Fig. 3. As concentrations increased of tartrate, the conductivity of the sodium tartrate increased so that the ultimate voltage would decrease. Thus as the concentration increased, the better conductivity of the sodium tartrate led to more ion's migration to the surface of the alloy substrate so that the rate of the formation of the anodic oxide film would be increased, leading to thicker anodic oxide film. In addition of the decreasing ultimate voltage and dissolution of anodic oxide film, the thickness of the anodic oxide film increased with the concentrations until the concentration reached 15 g/L, and then would no longer increase ultimately.

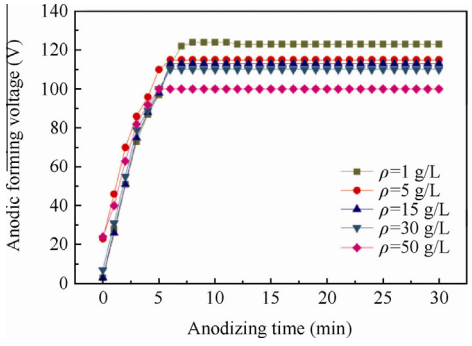

Fig. 3 Anodizing forming voltage with anodizing time relation curves of specimens at different electrolyte concentrations.

3.2. *Effect of concentrations on morphology*

Fig. 4 shows the scanning electron images of the surface of anodic oxide film obtained at different concentrations of sodium tartrate.

The anodic oxide film presented a uniform petaloid drum and micro-cracks morphology. The results of Fig. 4 indicate that PTFE particles were enriched on the surface of anodic oxide film and preferentially concentrated within internal micro-cracks of the film, which was in the circle shown in Fig. 4(c), that obviously improved the corrosion resistance of anodic oxide film. The petaloid drums showed in Fig. 4(a) were probably owe to different rates of the growth of different places due to different topographic features at different zones.[6] The anodic oxide film would be firstly formed as barrier layer and then the barrier layer ruptured because of the high voltage. And outer layer would be preferably formed at the defects of the surface. As the anodization continued, the thickness of the anodic oxide film was bigger and bigger at defects of the surface than other places. And the petaloid drums and micro-cracks appeared due to the internal pressure of the anodic oxide film.

The results of Fig. 4 indicate the presence of anodic oxide film on all the samples. As concentrations increased, the surfaces of the anodic oxide film became smoother. According to Fig. 4(a), when the concentration was less than 5 g/L, the anodic oxide film obtained was uncompact with the existence of the petaloid drums. The results of Fig. 4(b) indicate the presence of electron transport channels appearing as circular

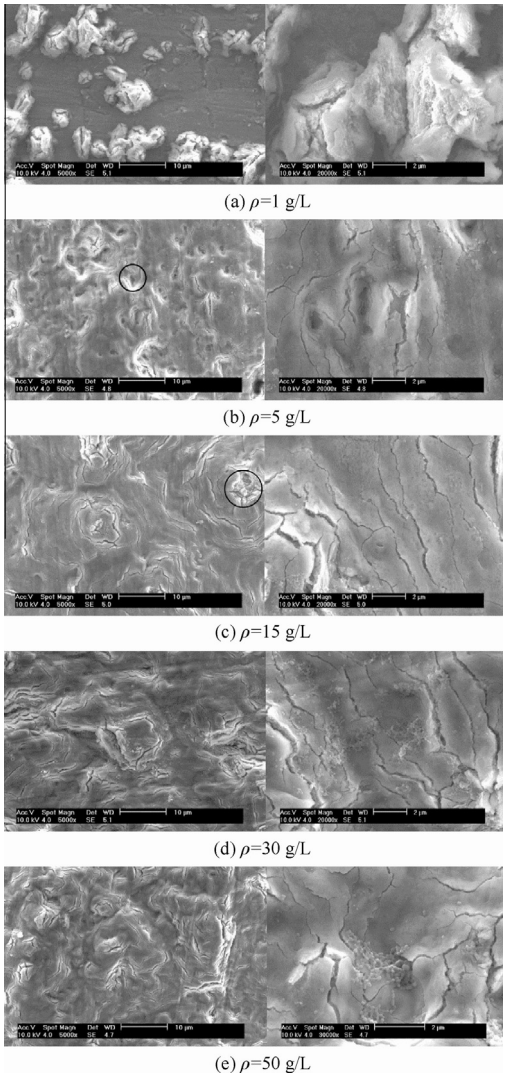

Fig. 4 SEM of anodic oxide film surface obtained at different concentrations of sodium tartrate.

spots distributed over the surface of the anodic oxide film when the concentration of sodium tartrate was 5 g/L. However, the electron transport channels were almost covered when the concentration increased to 15 g/L and translated to petaloid drums. As shown in Fig. 4(c–e), the anodic oxide film obtained at concentrations of sodium tartrate more than 5 g/L were compact. As concentrations increased, the number of the petaloid drums increased; on the other hand, the micro-cracks were dramatically swelling.

The EDS were also detected by using the function of scanning electron microscopy. Fig. 5 reveals the distribution of O, Ti and V along the yellow line (Fig. 5(a)). It was obvious that the content of O of petaloid drums exceeded other places, indicating that the petaloid drums, preferentially formed anodic oxide film, were composed of oxide. Moreover, the distribution of V, representatives of the alloying element, presented an opposite consequence. It was the results of the presence of anodic oxide film at the surfaces of substrates, decreasing the content of alloying element.

Fig. 6 shows the AFM three-dimensional topographic representations for the samples at different concentrations.

The average roughnesses of the surfaces calculated from the AFM images are shown in Fig. 7. It was obvious that the surface become rougher with the concentrations until the concentration reached 15 g/L, and then tended to be smoother morphology, in accordance with the results of SEM.

According to Fig. 7, the corresponding roughness values of the anodic oxide film are 66.3, 275, 320, 236, 294 nm respectively, when the concentrations are 1, 5, 15, 30, 50 g/L. The roughness value increased with increased concentrations until it reached 15 g/L, and then the roughness value reduced with increased concentrations. According to the SEM images, the sizes of the petaloid drums increased with increased concentrations. It was obvious that the size of the petaloid drums would affect the roughness value significantly. But when the concentration was more than 15 g/L, the roughness value reduced with increased concentrations. It was probably because of the compaction of the anodic oxide film. On the other hand, the roughness value of the surface formed in 1 g/L was remarkably low. It might be due to the imperfection of the anodic oxide film and the smaller size of the petaloid drums. When the concentration of the sodium tartrate was less than 5 g/L, the effect of the concentrations on the size of the petaloid drums would be researched in details.

3.3. Effect of concentrations on crystalline structure

To investigate the chemical states of Ti, the surface of the anodic oxide film was observed by a Raman micro-scope. The Raman spectra of the anodic oxide film fabricated at different concentrations are shown in Fig. 8. The results of Raman analysis illustrate a similarity in the crystal structure of the obtained Ti–10V–2Fe–3Al anodic oxide film with increased concentrations, consisting of mainly amorphous TiO_2, some anatase TiO_2 and a small amount of rutile TiO_2.

An obvious intense band at 152 cm^{-1} was very sharp which represented anatase and another obvious intense band of the anodic oxide film was detected at 632 cm^{-1} which represented rutile.[21] It was apparent that the anodic oxide film fabricated at different concentrations would have the same peaks. Furthermore, the intensity of the peaks increased with increased concentration until it reached 15 g/L. The intensity of the peaks would be related to the thickness of anodic oxide film that the thicker layer leaded to high intensity. Consequently, the anodic oxide film fabricated at different concentrations had the same crystal structure (anatase and rutile), well the intensity of TiO_2 anatase and TiO_2 rutile increased with the increase of concentration until it reached 15 g/L. And the ratio of anatase TiO_2 and rutile TiO_2 increased with the concentrations until the concentration was 15 g/L. The Raman spectra of the anodic oxide film fabricated at different concentrations indicate that the increase of the concentrations would promote the transformation from rutile TiO_2 to anatase TiO_2 while affecting the thickness of anodic oxide film, also in accordance with SEM, AFM.

3.4. Effect of concentrations on corrosion resistance

The polarizing curves of the anodic oxide film are shown in Fig. 9. The concrete data are given in Table 3.

Obviously, the corrosion current density i_{corr} of the anodic oxide film decreased with increased concentrations before 30 g/L, and then increased with further increased concentrations.

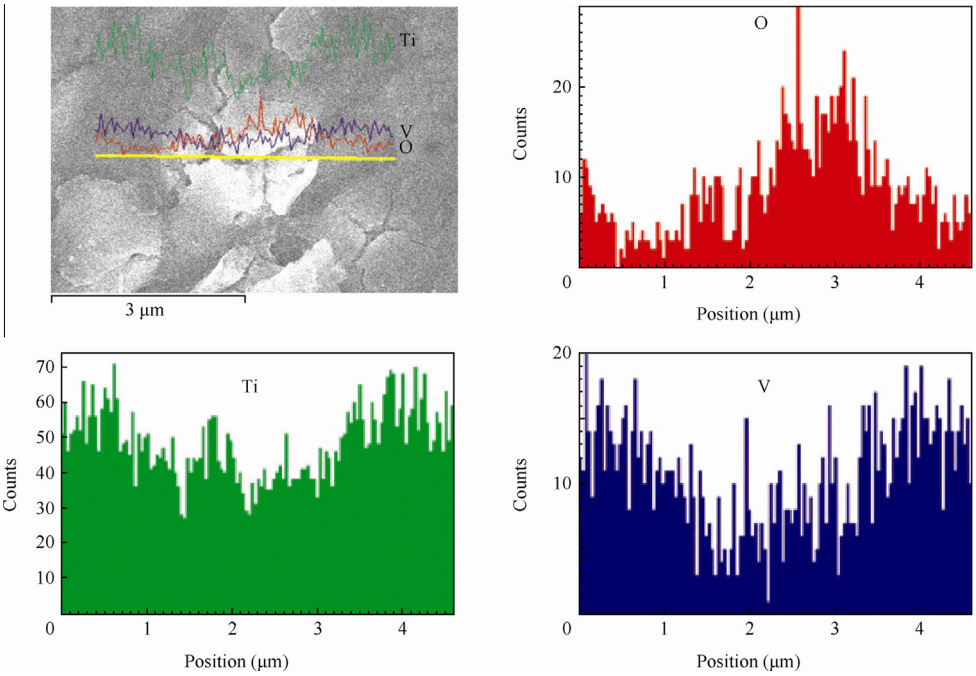

Fig. 5 EDS of anodic oxide film obtained when concentration is 1 g/L.

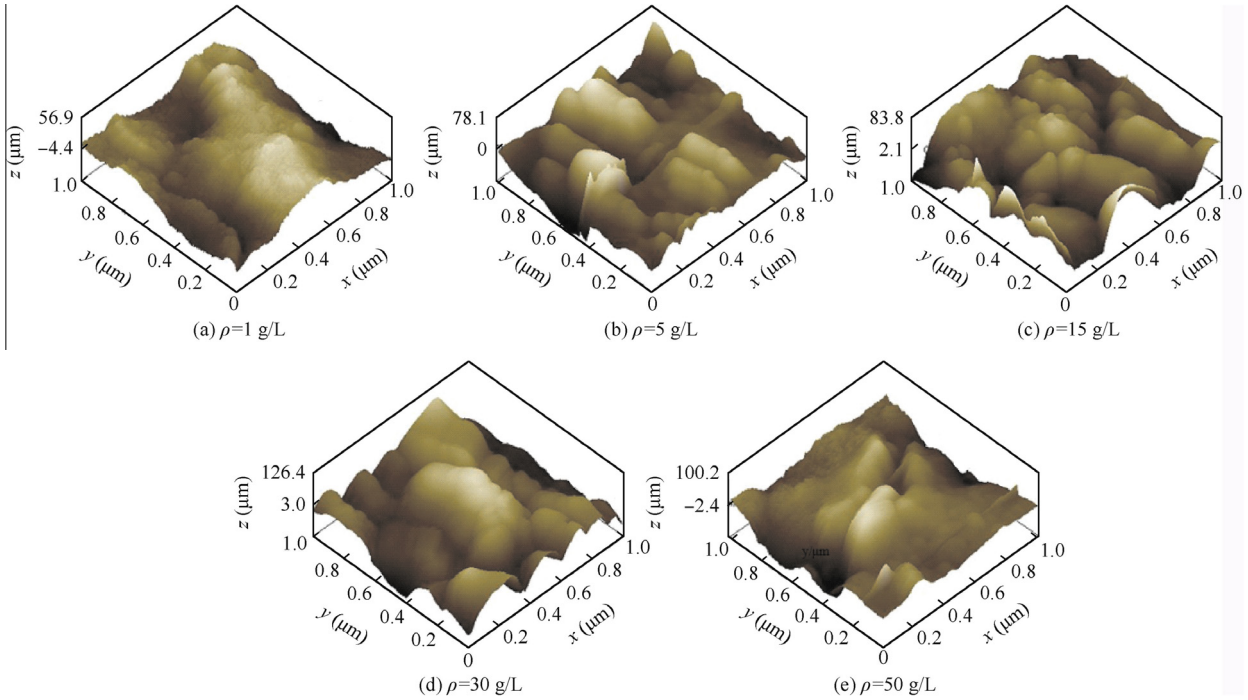

Fig. 6 AFM of three-dimensional anodic oxide film obtained at different concentrations of sodium tartrate.

According to polarizing curves and Table 3, the anodic oxidation potential processing would raise the E_{corr} as the concentration increased, and reached the maximum at 15 g/L, and then depressed as the concentration further increased. The nyquist diagram of the anodic oxide film in a 3.5% NaCl solution are shown in Fig. 10 to illustrate the corrosion resistance of anodic oxide film. The Z_{re} in Fig. 10 expresses resistance which is constant regardless of frequency, and the Z_{im} expresses reactance which varies with frequency due to capacitance and inductance.

The nyquist diagrams presented quadrants for all samples indicating the presence of anodic oxide film which was

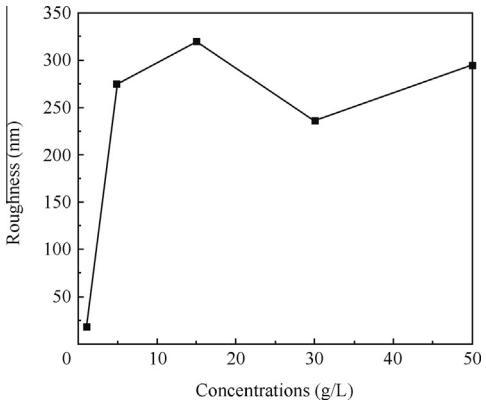

Fig. 7 Roughness of anodic oxide film fabricated at different concentrations.

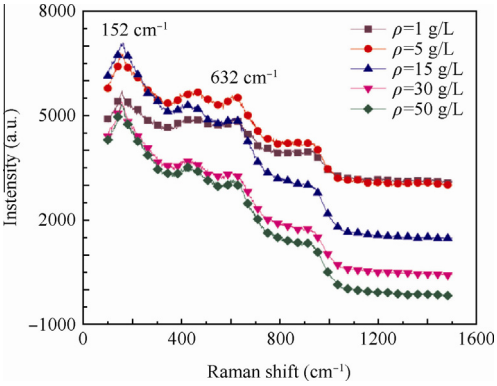

Fig. 8 Raman spectra of anodic oxide film fabricated at different concentrations.

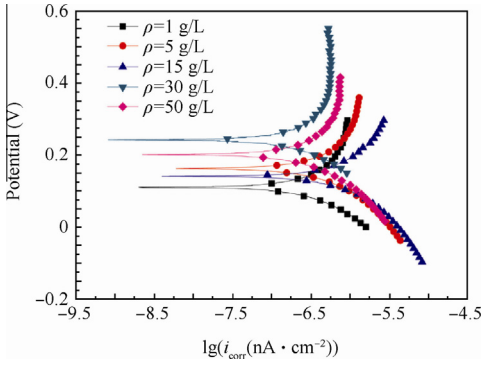

Fig. 9 Polarizing curves of anodic oxide film at different concentrations.

insulative. The radius of quadrants increased with increased concentrations before 15 g/L, and then decreased with further increased concentrations, consistent with the results of polarizing curves.

In general, the corrosion resistance of the anodic oxide film would be mainly related to the thickness, the surface states and

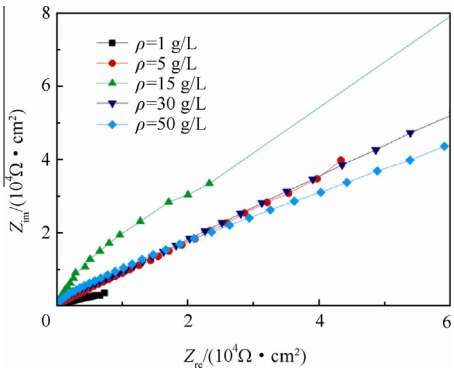

Fig. 10 Nyquist diagram of anodic oxide film at different concentrations.

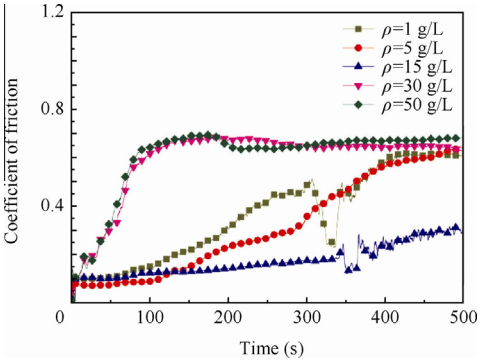

Fig. 11 Coefficient of friction of anodic oxide film at different concentrations.

structure of the anodic oxide film.[22] As anodic oxide film had the same crystal structure in the experiment, the key factors would then be the thicknesses and the surface states. According to Fig. 4, as the concentrations increased, the number and the sizes of the petaloid drums increased, and the anodic oxide film would be more compact. It was agreed with the results of the electrochemical measurement. And when the concentrations were more than 15 g/L, micro-cracks would be dramatically swelling, leading to the decrease of corrosion resistance.

3.5. Effect of concentrations on friction coefficient

The coefficients of friction of the anodic oxide film fabricated at different concentrations are shown in Fig. 11. All samples show a low coefficient of friction at the beginning of the test, and then increased, indicating the exposure of the Ti substrate.

It was obvious that the coefficient of friction of the anodic oxide film would reduce with the concentrations until it reached 15 g/L, then increase as concentrations increased. It was related to the morphology of the anodic oxide film and the enrichment of PTFE particles. As concentrations increased, the surfaces of the anodic oxide film became smoother, leading to lower coefficient of friction. In addition, PTFE particles were enriched on the surface of anodic oxide film and preferentially concentrated within internal microcracks that would increase with the concentrations. The PTFE

Table 3 Properties of anodic oxide film fabricated at different concentrations.

Concentration (g/L)	E_{corr} (V)	i_{corr} ($\mu A \cdot cm^{-2}$)
1	0.129	6.914×10^{-7}
5	0.215	4.272×10^{-7}
15	0.157	4.164×10^{-7}
30	0.185	1.657×10^{-7}
50	0.171	4.023×10^{-7}

particles would concentrate within internal micro-cracks which played a role of lubrication during the test until the Ti substrate exposed. On the other hand, when the concentration reached 30 g/L, the coefficient of friction of the anodic oxide film would increase because of the progress of the growth of the film. When the concentrations were more than 15 g/L, the rate of corrosion increased so that the film were loose, leading to the higher coefficient of friction. Though the thickness was similar when the concentrations are 5 g/L and 50 g/L, the time that the Ti substrate exposed was different. The Ti substrate exposed at about 80^{th} s when the concentrations were 30 g/L and 50 g/L, indicating worse wear resistance of the anodic oxide film.

3.6. Mechanism of concentrations' effect

In conclusion, the sodium tartrate would influence the properties of the anodic oxide film as the carrier of the electron. Because of the alternating current, the $(C_4O_6H_4)^{2-}$ would migrate into the oxide film from the solution while the Ti^{4+} migrate into the oxide film from the substrate. The oxide film would be formed with the migration of ions. Thus, at the early stage of the anodization, the barrier layer was formed firstly which was insulative and compact. And then, as the anodization continued, some defects of the surface appeared on the surface of the barrier layer so that the rounded outer layer would be formed afterwards at the defects of the surface. Ultimately, the rounded outer layer would touch and cover each other at different places of the surface of barrier layer as the size of outer layer increased. Hence, the petaloid drums would be formed due to the stress of the extrusion of inhomogeneous outer layer. At this stage, the O_2 gases would be formed and the size of the petaloid drums would increase, leading to the overloading of the stress of the surface of the petaloid drums. Then micro-cracks would be formed and the PTFE particles would preferentially migrate into the micro-cracks because of the adsorption. Thus the PTFE particles would preferentially concentrate within internal micro-cracks of the film.

As concentrations of tartrate increased, the resistance of the sodium tartrate would decrease, so that the electroconductivity of the sodium tartrate would be improved. At the beginning of the anodization, more $(C_4O_6H_4)^{2-}$ migration to the substrate led to more chances of the breaking of the barrier layer where the petaloid drums appeared, so that the number of the petaloid drums would increase as concentrations increased (Fig. 4). It was consistent with the results of Fig. 6 and Fig. 7 that the oxide film would become smoother as concentrations increased before 15 g/L. As the concentrations further increased, better electroconductivity would lead to the corrosion of the formed anodic oxide film. When the concentrations were more than 15–30 g/L, the rate of corrosion would be larger than the rate of formation, and the thicknesses of the anodic oxide film would decrease. The micro-cracks of the film that were exposed by the corrosion of the concentration contributed to the average roughness and the smoothness. It also contributed to the decrease of the corrosion resistance and wear resistance of the anodic oxide film when the concentrations were more than 15 g/L (Table 3 and Fig. 11).

4. Conclusions

(1) The sodium tartrate would influence the properties of the anodic oxide film as the carrier of the electron. Thus, the thicknesses would be related to the rates of formation and dissolution of the anodic oxide film at different concentrations.
(2) The presence of the petaloid drums would be related to different rates of formation of anodic oxide film at different places. As concentrations increased, more $(C_4O_6H_4)^{2-}$ migration to the substrate would offer more chances of the formation of the oxide film at the beginning of the anodization, leading to more petaloid drums and smoother surfaces of the anodic oxide film.
(3) PTFE particles would preferentially concentrate within internal micro-cracks of the film because of the adsorption.
(4) The micro-cracks of the film that were exposed by the corrosion of the concentration would contribute to the average roughness, smoothness, corrosion resistance and wear resistance of the anodic oxide film.

Acknowledgements

The authors thank the anonymous reviewers for their critical and constructive review of the manuscript. This study was supported by the National Natural Science Foundation of China (No. 51271012).

References

1. Capek D, Gigandet MP, Masmoudi M, Wery M, Banakh O. Long-time anodisation of titanium in sulphuric acid. *Surf Coat Technol* 2008;**202**(8):1379–84.
2. Kumar S, Sankara N, Saravana K. Influence of fluoride ion on the electrochemical behaviour of β-Ti alloy for dental implant application. *Corros Sci* 2010;**52**(5):1721–7.
3. Neupane MP, Park IS, Lee SJ, Kim KA, Lee MH, Bae TS. Study of anodic oxide films of titanium fabricated by voltammetric technique in phosphate buffer media. *J Electrochem Soc* 2009;**4**(2):197–207.
4. Frayret JP, Caprani RP. Anodic behaviour of titanium in acidic chloride containing media (HCl-NaCl). Influence of the constituents of the medium-I. Study of the stationary current. Calculation of the overall reaction orders. *Electrochim Acta* 1981;**26**(12):1783–8.
5. Duarte LT, Bolfarini C, Biaggio SR, Rocha-Filho RC, Nascente PA. Growth of aluminum-free porous oxide layers on titanium and its alloys Ti–6Al–4V and Ti–6Al–7Nb by micro-arc oxidation. *Mater Sci Eng C* 2014;**41**(1):343–8.
6. Fan M, Mantia FL. Effect of surface topography on the anodization of titanium. *Electrochem Commun* 2013;**37**:91–5.

7. El-Mahdy G, Kim KB. Monitoring the atmospheric corrosion loss of copper during wet/dry cyclic conditions in oxalic acid solutions. *Corrosion* 2007;**63**(2):171–7.
8. Ohtsuka T, Masuda M, Sato N. Ellipsometric study of anodic oxide films on titanium in hydrochloric acid, sulfuric acid, and phosphate solution. *J Electrochem Soc* 1985;**132**(4):787–92.
9. Wang D, Li H, Yang H, Ma J, Li G. Tribological evaluation of surface modified H13 tool steel in warm forming of Ti–6Al–4V titanium alloy sheet. *Chin J Aeronaut* 2014;**27**(4):1002–9.
10. Liu JH, Yi JL, Li SM, Yu M, Wu GL, Wu L. Effect of electrolyte concentration on morphology, microstructure and electrochemical impedance of anodic oxide film on titanium alloy Ti–10V–2Fe–3Al. *J Appl Electrochem* 2010;**40**(8):1545–53.
11. Ohtsu N, Ishikawa D, Komiya S, Sakamoto K. Effect of phosphorous incorporation on crystallinity, morphology, and photocatalytic activity of anodic oxide layer on titanium. *Thin Solid Films* 2014;**556**:247–52.
12. Ohtsu N, Komiya S, Kodama K. Effect of electrolytes on anodic oxidation of titanium for fabricating titanium dioxide photocatalyst. *Thin Solid Films* 2013;**534**:70–5.
13. Liu JH, Yang K, Yu M, Li SM, Wu L, Yu XM. Preparation, characterization and fatigue properties of TC18 titanium alloy anodic oxide film in sodium hyaluronate system. *Acta Aeronaut Astronaut Sin* 2014;**35**(3):902–10 [Chinese].
14. Wu GL, Li SM, Yu M, Yi JL, Wu L. Surface analysis of chemical stripping titanium alloy oxide films. *J Wuhan Univ Technol-Mater Sci* 2012;**27**(3):399–404.
15. Komiya S, Sakamoto K, Ohtsu N. Structural changes of anodic layer on titanium in sulfate solution as a function of anodization duration in constant current mode. *Appl Surf Sci* 2014;**296**:163–8.
16. Ou SF, Chou HH, Lin CS, Shih CJ, Wang KK, Pan YN. Effects of anodic oxidation and hydrothermal treatment on surface characteristics and biocompatibility of Ti–30Nb–1Fe–1Hf alloy. *Appl Surf Sci* 2012;**258**(17):6190–8.
17. Tan Y. An overview of techniques for characterizing inhomogeneities in organic surface films and underfilm localized corrosion. *Prog Org Coat* 2013;**76**(5):791–803.
18. Li SM, Yu XM, Liu JH, Yu M, Wu GL, Wu L, et al. Influence of working frequency on structure and corrosion resistance of the anodic oxide film on Ti–6Al–4V alloy. *Int J Electrochem Sci* 2013;**8**(4):5438–47.
19. Habazaki H, Fushimi K, Shimizu K, Skeldon P, Thompson GE. Fast migration of fluoride ions in growing anodic titanium oxide. *Electrochem Commun* 2007;**9**(5):1222–7.
20. Ohsaka T, Izumi F, Fujiki YJ. Raman spectrum of anatase TiO_2. *J Raman Spectrosc* 1978;**7**:321.
21. Porto S, Fleury P, Damen T. Raman spectra of TiO_2, MgF_2, ZnF_2, FeF_2, and MnF_2. *Phys Rev* 1967;**154**(2):522.
22. Yu M, Liu YX, Liu JH, Li SM, Xue B, Zhang Y, et al. Effects of cerium salts on corrosion behaviors of Si–Zr hybrid sol–gel coatings. *Chin J Aeronaut* 2015;**28**(2):600–8.

Ma Kun received his B.S. degree from Shandong University in 2013 and M.S. degree from Beihang University, respectively. His main research interests are corrosion science and protection technology.

Yu Mei received her Ph.D. degree from Beihang University in 2007 and is now an associate professor of materials science and engineering at the same university. Her main research interests are nano functional materials, corrosion science and protection technology.